Gα$_s$-Biased β$_2$-Adrenergic Receptor Signaling from Restoring Synchronous Contraction in the Failing Heart

Khalid Chakir[1,*], **Charlene Depry**[2,*], **Veronica L. Dimaano**[1], **Wei-Zhong Zhu**[3], **Marc Vanderheyden**[4], **Jozef Bartunek**[4], **Theodore P. Abraham**[1], **Gordon F. Tomaselli**[1], **Shu-bai Liu**[5], **Yang K. Xiang**[5], **Manling Zhang**[1], **Eiki Takimoto**[1], **Nickolai Dulin**[6], **Rui Ping Xiao**[3], **Jin Zhang**[2], and **David A. Kass**[1,†]

[1]Division of Cardiology, Department of Medicine, Johns Hopkins University School of Medicine, Baltimore, MD 21205, USA

[2]Department of Pharmacology and Molecular Sciences, Johns Hopkins University School of Medicine, Baltimore, MD 21205, USA

[3]Laboratory of Cardiovascular Science, Gerontology Research Center, National Institute on Aging, National Institutes of Health, Baltimore, MD 21224, USA

[4]Cardiovascular Center, Onze Lieve Vrouwziekenhuis, 9300 Aalst, Belgium

[5]Molecular and Integrative Physiology and Neuroscience Program, University of Illinois at Urbana Champaign, Urbana, IL 61820, USA

[6]Department of Medicine, University of Chicago, Chicago, IL 60637, USA

Abstract

Cardiac resynchronization therapy (CRT), in which both ventricles are paced to recoordinate contraction in hearts that are dyssynchronous from conduction delay, is the only heart failure (HF) therapy to date to clinically improve acute and chronic function while also lowering mortality. CRT acutely enhances chamber mechanical efficiency but chronically alters myocyte signaling, including improving β-adrenergic receptor reserve. We speculated that the latter would identify

unique CRT effects that might themselves be effective for HF more generally. HF was induced in dogs by 6 weeks of atrial rapid pacing with (HF_{dys}, left bundle ablated) or without (HF_{syn}) dyssynchrony. We used dyssynchronous followed by resynchronized tachypacing (each 3 weeks) for CRT. Both HF_{dys} and HF_{syn} myocytes had similarly depressed rest and β-adrenergic receptor sarcomere and calcium responses, particularly the $β_2$-adrenergic response, whereas cells subjected to CRT behaved similarly to those from healthy controls. CRT myocytes exhibited suppressed $Gα_i$ signaling linked to increased regulator of G protein (heterotrimeric guanine nucleotide–binding protein) signaling (RGS2, RGS3), yielding $Gα_s$-biased $β_2$-adrenergic responses. This included increased adenosine cyclic AMP responsiveness and activation of sarcoplasmic reticulum–localized protein kinase A. Human CRT responders also showed up-regulated myo-cardial RGS2 and RGS3. Inhibition of $Gα_i$ (with pertussis toxin, RGS3, or RGS2 transfection), stimulation with a $Gα_s$-biased $β_2$ agonist (fenoterol), or transient (2-week) exposure to dyssynchrony restored β-adrenergic receptor responses in HF_{syn} to the values obtained after CRT. These results identify a key pathway that is triggered by restoring contractile synchrony and that may represent a new therapeutic approach for a broad population of HF patients.

INTRODUCTION

Despite major developments in both diagnosis and treatment, heart failure (HF) continues to be a leading cause of death and disability in older adults worldwide, affecting more than 12 million patients in the United States and Europe alone (1). Until recently, HF therapy usually consisted of pharmacological approaches to counter maladaptive neurohormonal stimulation and restore favorable hemodynamics. Over the past decade, however, the major advance has come from a device therapy termed cardiac resynchronization therapy (CRT) that uses electrical pacing of both right and left ventricles to restore contraction timing. It is designed to counter the dyssynchronous contraction within the left ventricle stemming from electrical conduction delay that is found in nearly a third of patients with HF. Electromechanical dyssynchrony confers independent risks for worsened morbidity and mortality, and CRT improves both in affected patients (2–5).

CRT is unique among HF treatments because it both acutely (6) and chronically (7) enhances systolic function of the heart yet confers long-term survival benefits (2, 3). None of the commonly used drugs designed to stimulate ventricular pump function has yet achieved this. Furthermore, although dyssynchrony worsens HF risk, once this is ameliorated by CRT, patient outcome is better than in individuals with less dyssynchrony to start with (8). This suggests that CRT might invoke unique myocardial changes not observed in HF with synchronous contraction. To date, knowledge of the molecular and cellular effects of CRT remains limited, because the therapy was developed in humans directly, and less than 0.5% of the >3000 published studies have examined basic mechanisms. To address this gap, we developed an experimental animal model of HF with dyssynchrony that we have treated with CRT, which has shown that CRT improves myocyte survival, restores regional homogeneity of molecular transcription and stress kinase activation (9, 10), enhances β-adrenergic responsiveness (11), and reverses electrophysiological maladaptations (12). These findings suggested that specific molecular modifications from CRT could be identified (a form of reverse engineering) that in turn could benefit HF more broadly, for example, in patients without dyssynchrony.

Here, we pursued this concept, focusing on the capacity of CRT to reverse depressed β-adrenergic–stimulated myocyte function and calcium handling.

RESULTS

Effect of synchronous, dyssynchronous, or resynchronized HF on regional wall motion and chamber function

To identify differences in β-adrenergic signaling between synchronous, dyssynchronous, and resynchronized HF, we used several variants of the tachypacing-induced HF canine model (11). Figure 1A displays examples of regional shortening (strains) determined by speckle tracking imaging for both anterior/septal and lateral walls in each model. Strains were synchronous in normal controls, whereas HF_{dys} had marked discoordination that was restored by CRT (biventricular pacing). Dyssynchrony was also generated by right ventricular (RV) free wall pacing and then resynchronized by reverting to atrial pacing (V3A3; Fig. 1A, lower left/middle). HF_{syn} (atrial pacing) had coordinated contraction throughout. Strain magnitude fell ~40% in all models from control levels (*y*-axis scales adjusted), indicating cardiac depression. Although dyssynchrony/synchrony history differed among models, all developed similar global systolic and diastolic dysfunction (fig. S1), because all were tachypaced for 6 weeks, and this had a dominant effect on the integrated hemodynamic response. Thus, molecular/cellular differences between the models reflected the specifics of synchronization history rather than systemic depression.

Effect of resynchronization on basal and isoproterenol-stimulated function and Ca^{2+}

The acute impact of β-adrenergic receptor (β-AR) stimulation on myocyte dynamics and whole-cell Ca^{2+} transients was determined in cells freshly isolated from each model. Rest and β-AR–stimulated (isoproterenol) sarcomere shortening and relengthening, and peak Ca^{2+} transient and decay rate, were markedly and similarly depressed in myocytes from always dyssynchronous or synchronous HF. Both features returned to control levels in the resynchronization models (Fig. 1, B and C). Thus, enhanced β-AR responsiveness did not reflect the presence of contractile synchrony but rather a history of dyssynchrony that was subsequently ameliorated.

Effect of resynchronization on β-AR density and $β_2$-AR G_i coupling

Differential β-AR signaling was in part due to a decline in combined $β_1$ and $β_2$ subtype receptor density in HF_{dys} and HF_{syn} that was ameliorated by resyn-chronization (Fig. 2A). Receptor affinity (both subtypes) was unaltered in all models (fig. S2). $β_1$ gene expression declined in HF_{dys}, and myocyte response to selective $β_1$ stimulation was depressed in this model and less so in HF_{syn} (fig. S3). Because both HF_{dys} and HF_{syn} had similar depressed responses to isoproterenol, we hypothesized that differential $β_2$-AR regulation may play a more prominent role in the depressed response to β-AR signaling in HF_{dys} and to its restoration with resynchronization.

$β_2$-AR signaling coactivates both stimulatory and inhibitory G proteins (heterotrimeric guanine nucleotide–binding proteins). To better understand this signaling, we stimulated cells with the $β_2$-selective agonist zinterol (1 μM) with or without the $Gα_i$ inhibitor pertussis toxin (PTX) (Fig. 2, B and C). PTX augmented zinterol-stimulated shortening and Ca^{2+} transients slightly in controls but greatly amplified the response in cells from HF_{dys} and HF_{syn}. In contrast, cells from resynchronized hearts had enhanced responses to zinterol that were little changed after PTX, indicating that the $β_2$-AR in these hearts was already biased toward $Gα_s$-coupled signaling. To further test this, we treated cells with the *R,R*-enantiomer of fenoterol, a biased $β_2$ agonist that does not activate $Gα_i$ protein (13). As shown in Fig. 2C, all HF models now had similar responses to fenoterol, with somewhat higher Ca^{2+} transients in CRT/V3A3 groups. This was similar to zinterol + PTX responses in all groups and augmented over zinterol alone in HF_{dys} and HF_{syn}. Fenoterol and zinterol responses were

similar in the resynchronization models. These data show that a history of dyssynchrony followed by resynchronization uniquely generates a $G\alpha_s$-biased β_2-AR.

Biased β_2-AR signaling is coupled with enhanced cAMP generation and protein kinase A activity at the sarcoplasmic reticulum

To further clarify the nature of the altered β_2-AR signaling, we performed studies in isolated myocytes infected with an adenovirus containing a plasma membrane–targeted adenosine 3′, 5′-monophosphate (cAMP)–sensitive fluorescence resonance energy transfer (FRET) probe (ICUE3) based on the EPAC1 (exchange protein directly activated by cAMP 1) binding domain (Fig. 3A) (14). After 24 hours, cells were stimulated with either zinterol or fenoterol, each in the presence of a broad-spectrum phosphodiesterase (PDE) inhibitor, IBMX. Zinterol-stimulated cAMP increase in both resynchronization models exceeded that in the other groups (including control). In contrast, all responded similarly to fenoterol (Fig. 3C, including summary), as had been observed with sarcomere shortening. This indicated that $G\alpha_s$-coupled signaling was not blunted in these models, but rather, there was bias away from $G\alpha_i$ coupling. Because PDEs were broadly inhibited, the results support differential cAMP generation rather than hydrolysis.

Previous studies have proposed that reduced $G\alpha_i$ coupling to the β_2-AR can modify the targeting of cAMP, resulting in enhanced protein kinase A (PKA) activation of sarcoplasmic reticulum (SR) calcium-handling proteins and thus augmentation of the Ca^{2+} and associated myocyte shortening (15). Attempts to identify compartmentalized cAMP signaling in the canine myocytes using targeted FRET probes proved unsuccessful, but we were able to infect cells with a virus containing a FRET-based PKA activity reporter (AKAR3) target to the SR (16) (Fig. 3D). In myocytes from HF_{dys} or HF_{syn}, zinterol resulted in negligible PKA stimulation detected at the SR, whereas in CRT cells, activation was detectable (Fig. 3F). As a control, we used fenoterol and detected PKA activation in cells from all models (fig. S4).

Effect of resynchronization on β-AR–coupled and –regulating proteins

Depression of β-adrenergic stimulatory signaling in HF has been linked to up-regulation of G_i expression (17–19) and G receptor kinase 2 (GRK2) (20), the latter coupled to β-AR desensitization by internalization and degradation. Both were observed in HF_{dys} and HF_{syn} models (Fig. 4, A and B) but were similarly enhanced in both resynchronization models. $G\alpha_s$ expression was unaltered between models and versus normal controls. We also performed analysis of β-arrestin1 and β-arrestin2 expression, but there were no consistent differences between models (fig. S5). Another mechanism to regulate $G\alpha_i$ proteins is via regulators of G protein–coupled signaling (RGS), whose canonical role is as guanosine triphosphatase (GTPase)–activating proteins (GAPs) to reverse α subunit activity. In heart muscle, RGS3 and RGS4 are recognized to target $G\alpha_i$. Although RGS2 is thought to more prominently target $G\alpha_q$, recent evidence also supports $G\alpha_i$ regulation, so we examined all three forms. As shown by Western blot analysis (Fig. 5, A and B), HF_{syn} and HF_{dys} expressed low levels of RGS2/3 protein, similar to controls, but both were up-regulated in each of the resynchronization models. In contrast, RGS4 was not significantly altered. RGS3 expression shown in Fig. 5 reflected the long form (~70 kD), but differential expression was observed in the short form (~25 kD) as well (fig. S6).

Changes in RGS2/3 protein expression were mirrored by gene expression (fig. S7), suggesting that they might provide a biomarker of CRT response. To test this, we determined mRNA expression from left ventricular (LV) myocardial biopsy specimens obtained in 15 HF patients with dyssynchrony at baseline and 4 months after initiating CRT. All had idiopathic dilated cardiomyopathy (12 men), with mean age of 66 ± 2 years, New York Heart Association (NYHA) symptom score of 3.4 ± 0.1, QRS duration of 158 ± 4 ms,

and resting ejection fraction (EF) of $22.1 \pm 1.5\%$. Of these patients, nine were clinical responders (relative increase in EF of 20% or more and fall in functional class >1) (21), and in these patients, RGS2 and RGS3 expression increased significantly, whereas this was not observed in nonresponders (Fig. 5C). Thus, enhanced RGS2/3 expression is also observed in humans receiving CRT who demonstrate clinical benefit. There were no disparities or changes in gene expression of $G\alpha_i$ or β-arrestin2 in these same patients.

RGS2/3 up-regulation is sufficient to explain biased β₂ response in resynchronized models

To test whether up-regulation of either RGS2 or RGS3 is sufficient to explain differential β_2 responses, we isolated and infected myocytes from HF_{dys}, HF_{syn}, and CRT with adenovirus expressing green fluorescent protein (GFP) (control) or wild-type RGS2 or RGS3 (Fig. 6A). Transfection with GFP did not alter RGS expression, but levels increased two- to threefold in isolated myocytes, similar to that observed in vivo. Cell function and Ca^{2+} handling were studied after 24 hours, and we found that up-regulation of RGS2 or RGS3 enhanced sarcomere shortening and peak Ca^{2+} response to zinterol, similar to that with zinterol + PTX (Fig. 6B). There was no further augmentation by combining RGS2 or RGS3 infection with PTX, indicating that targeting was likely similar.

Transient dyssynchrony in synchronous HF induces Gαₛ-biased β₂-AR signaling

Our finding that restoring synchrony from a dyssynchronous HF state was required to induce the changes in β_2-AR signaling led us to the following hypothesis: Might transient exposure to dyssynchrony in otherwise synchronous HF induce a similar response? If so, this would suggest that the seeming paradoxical therapy of transient RV pacing might improve adrenergic responsiveness in HF_{syn}. To test this, we exposed dogs ($n = 5$) sequentially to atrial, RV, and then atrial tachypacing, each for 2 weeks (model referred to as AVA); the only difference between HF_{syn} and AVA was the middle 2-week period. Global heart function at 6 weeks was similar to the other HF models (for example, EF, ~30%; end-diastolic pressure, 33 mmHg; dP/dt_{max}/IP, 16 s^{-1}). As shown in Fig. 7A, isoproterenol-stimulated shortening, relaxation, and peak calcium in AVA myocytes were similar to that from CRT hearts. AVA cells also responded robustly to zinterol, which was not further altered by PTX, in contrast to HF_{syn} behavior (Fig. 7B). Unlike CRT, neither RGS2 nor RGS3 expression increased in the AVA model (Fig. 7C). RGS4, $G\alpha_i$, GRK2, and β-arrestin1 expression were also similar (fig. S8) to levels observed in the other HF models (fig. S8). However, we observed a substantial decline in β-arrestin2 in AVA, below that in the other HF models and in controls (Fig. 7D). Because β-arrestin can switch β_2-AR signaling toward $G\alpha_i$-coupled cascades (22), this change might be related to the loss of such coupling with AVA.

DISCUSSION

Despite the overall clinical success of CRT over the past decade, cellular and molecular mechanisms by which it confers sustained benefits are only recently being revealed. Identifying these mechanisms offers an opportunity to apply changes induced by CRT to a broader HF population without involving biventricular stimulation. The present study advanced this goal in several ways. First, we show that depressed myocyte function, calcium handling, and β-AR responsiveness in synchronous or dyssynchronous HF are much improved in hearts that were first dyssynchronous and later resynchronized. Second, we identify that a major change underlying adrenergic reserve is $G\alpha_s$-biased β_2-AR signaling ($G\alpha_i$ decoupling) that enhances cAMP activation and stimulation of PKA within the SR, improving cell Ca^{2+} cycling and contraction. This modification is coupled to enhanced RGS2 and RGS3 expression, changes also found in humans responsive to CRT. A similar improvement in rest and β-AR response was achieved by temporarily rendering contraction

dyssynchronous by RV pacing, although here the molecular mechanism may differ, potentially involving β-arrestin2 modification. These results identify a key signaling change from CRT that could potentially benefit all forms of HF either by cardiac-targeted RGS2/3 enhancement or by novel uses of traditional ventricular pacing.

Members of the RGS superfamily are ubiquitously expressed in all cells, and in the heart, RGS1 to RGS7, RGS9, RGS12, and RGS14 are all expressed at the mRNA level (23). RGS2 (24, 25), RGS4 (26, 27), and, recently, RGS5 have been studied in genetic gain- or loss-of-function models; their deficiency exacerbates maladaptive remodeling in hearts subjected to stresses such as sustained pressure overload. RGS6 is prominently expressed in sinoatrial and atrioventricular nodal tissue and is involved with cardiac parasympathetic activation (28). Nothing as yet has been reported for cardiac RGS3, although it is expressed and up-regulated in response to G_q-coupled agonists (24) in vitro. Myocyte targeting of both $G\alpha_q$ and $G\alpha_i$ has been reported with each of these RGS proteins, and the primary mechanism for this is consistent with their GAP function. Noncanonical regulation has also been reported involving direct interaction of RGS proteins with Gβγ, adenylate cyclase (AC), phosphatidylinositol 3-kinase (PI3K), transforming growth factor–β (TGF-β) signaling, and protein synthesis (29). For example, RGS2 and RGS3 inhibition of AC does not appear to involve GAP activity against G_s protein (30, 31) but rather to target RGS-AC protein interaction via critical residues outside the RGS domain.

The present findings support potent regulation by either RGS2 or RGS3 against $G\alpha_i$ coupling, but not $G\alpha_s$ or AC, given that both the in vivo and the in vitro studies involving RGS2/3 up-regulation demonstrated enhanced $G\alpha_s$ receptor–coupled signaling (both functionally and by cAMP and PKA measurement). Evidence that RGS can regulate β_2-AR has been reported using mice expressing a mutant $G\alpha_i$ insensitive to RGS regulation (32). A number of previous studies have suggested that cardiac G_i activation confers cytoprotection that is coupled to extracellular signal–regulated kinase (ERK) (33) and/or PI3K activation (34). Thus, the decline in G_i-coupled signaling with CRT might raise concerns of the opposite behavior. However, CRT has been shown to reduce apoptosis in experimental models (10) and in humans (35), associated with enhanced survival signaling coupled to Akt and BAD (10).

Although RGS2 has been considered to primarily target $G\alpha_q$ rather than $G\alpha_i$, it binds to the β_2-AR, with the chaperone protein spinophilin playing a key role (36), and this could affect targeting in vivo. We recently showed that enhanced β_2-AR responsiveness in cultured myocytes (grown without adrenergic stimulation) was due to RGS2, further confirming this role by both gain- and loss-of-function analysis (37). RGS2 suppression of G_q signaling could also alter β_2-AR regulation by receptor (38) or GRK2 (39) phosphorylation by protein kinase C (PKC), and inactivation of adenylyl cyclases by calmodulin kinase. The present study translates these earlier cell-based studies regarding RGS2/3 modulation of β_2-ARs to the intact heart, and this type of change appears unique to CRT; it has not been reported from other HF therapies.

The marked disparity between the HF_{syn} and V3A3 and AVA models is intriguing. In the case of V3A3, the difference stemmed from what occurred during the initial 3 weeks (dyssynchrony versus synchrony), whereas for the AVA model, dyssynchrony was induced after 2 weeks of atrial pacing and HF induction, shortening the dyssynchrony exposure further. Both support the notion that exposure to and then reversal of dyssynchrony is required to induce the β-AR signaling change, and this does not require biventricular stimulation (traditional CRT). The modifications induced by dyssynchrony that lead to improved rest and β-AR reserve after its resolution remain under investigation, although this is not the first suggestion that short-term dyssynchrony pacing could have beneficial

myocardial effects. In one study, Vanagt and colleagues (40) reported that repetitive exposure to 5 min of RV pacing induced ischemic preconditioning protecting the heart against subsequent infarction. In another, pacing after infarction improved out-come linked to stimulation of K_{ATP} (adenosine triphosphate–sensitive potassium) channels and PKC pathways (41). It seems likely that changes related to regional mechanical loading and timing of stress development, coupled to restoration of synchrony, are important to the current responses. However, the cellular and molecular changes are global, as is enhanced β-AR signaling, so the impact of the mechanics is broader.

Our results suggest several methods to potentially translate benefits from CRT to HF patients who are otherwise not candidates and/or respond poorly to CRT. One is that CRT in general may be enhanced by intermittently using RV pacing to stimulate molecular signaling changes that are subsequently and beneficially modified by reinstating CRT. This might enhance effects in CRT nonresponders. More provocatively, the AVA data suggest that one might purposely induce dyssynchrony by RV pacing in synchronous HF for a limited duration (weeks to a few months) and then revert to normal sinus. Many HF patients receive implantable defibrillators to counter a high risk of sudden death, and these systems could be easily modified for this purpose. Enhancement of RGS2 or RGS3 in the heart would probably require myocyte targeting given their ubiquitous expression in multiple cell types. Adeno-associated virus gene transfer methods are being tested for clinical heart disease (42), and this might be further developed. Last, fenoterol as a mixture of *R,R*-enantiomer and *S,S*-enantiomer was first developed for asthma, but worsened death (43). However, the use of the *R,R*-enantiomer alone for heart disease was never examined and may still prove a viable treatment.

The current study did not identify mechanisms by which CRT up-regulates RGS2/3 [or, for the case of transient dyssynchrony exposure (AVA), suppressed β-arrestin2]. We did show that direct myocardial stimulation is not required, because recovery of contractile synchrony through the intrinsic His-Purkinje system was equally effective as bi-ventricular pacing. The fact that the changes are global points to an integrative signal rather than one specific to a regional stress and strain disparity. We also could not prove the centrality of RGS up-regulation to achieve CRT efficacy, although our data did show it was sufficient to achieve the primary change in β-adrenergic behavior in myocytes. Addressing these questions will be difficult, because there are no in vitro models of CRT, but may be helped by development of a mouse CRT model now under way.

In summary, we provide evidence that the $β_2$-AR becomes un-coupled from G_i proteins in dyssynchronous failing hearts that are subsequently resynchronized, potently contributing to systolic reserve. This is not observed in HF where contraction is either always synchronous or always dyssynchronous. Whether achieved by pacemaker-induced transient dyssynchrony or by up-regulation of RGS2/3 proteins, the improved reserve can be induced in other forms of HF. These findings suggest new avenues for pharmacological or pacing treatments to treat this increasingly common disease.

MATERIALS AND METHODS

HF models

Five rapid-pacing models of HF were studied. Dyssynchronous HF (HF_{dys}, *n* = 16) dogs were first subjected to left bundle radio-frequency ablation followed by 6 weeks of atrial tachypacing (200 min^{-1}). Always synchronous HF (HF_{syn}, *n* = 13) also underwent atrial tachypacing, but without previous LBB ablation. Two models of CRT were studied. One started as HF_{dys} for 3 weeks, then switched to 3-week biventricular tachypacing (LV lateral and RV anteroapical epicardium) (CRT, *n* = 14). The other started with RV tachypacing for

3 weeks to induce dyssynchronous HF, then switched to atrial pacing (V3A3, *n* = 11) for 3 weeks. A fifth group was exposed to atrial, RV, then atrial tachypacing (each 2 weeks, AVA, *n* = 5). Last, healthy normal controls were studied (*n* = 17). Controls ± sham surgery behave identically (11). Echo-cardiography and tissue Doppler (longitudinal strain speckle tracking with four-chamber views) were performed at 3 and 6 weeks to assess dyssynchrony (variance of peak systolic strain timing) as described (11). At terminal study, dogs were anesthetized with pentobarbital, pacing was suspended, and a micromanometer (Millar Instruments Inc.) was advanced to record LV pressure. The chest was opened and hearts were rapidly harvested under cold cardioplegia, with the myocardium frozen for tissue analysis or prepared for myocyte isolation (11).

Myocyte function studies

Myocyte sarcomere shortening and whole-cell calcium transients were assessed with an inverted microscope (Ellipse TE2001, Nikon) equipped with an image-fluorescence system (MyoCam, IonOptix). Myocyte function studies were performed at 37°C and paced by field stimulation at 1 Hz, as described (11).

Protein and gene expression

Myocardium was homogenized in lysis buffer (Cell Signaling Technology), and 50 to 100 μg were loaded for gel electrophoresis with standard methods. $G_i(1,2,3)$, G_s, RGS2, RGS3, RGS4, GRK2, and β-arrestin1/2 (Santa Cruz Biotechnology; each at 1:400) and glyceraldehyde-3-phosphate dehydrogenase (GAPDH) (Imgenex; 1:10,000) were probed. Gene expression was assessed by real-time polymerase chain reaction (PCR) with the SYBR Green PCR master mix (Applied Biosystems) and ABI Prism 7900.

Radioligand binding assay

β-AR radioligand binding studies were performed using myocardial membrane fractions with the nonselective β-AR antagonist [^{125}I]-labeled cyanopindolol, as described (44).

Myocyte culture and adenoviral infection

Isolated myocytes were washed three times with minimum essential medium (MEM) containing 1.2 mM Ca^{2+}, 2.5% fetal bovine serum (FBS), and 1% penicillin-streptomycin, and then plated with the same medium in culture dishes precoated with mouse laminin (10 μg/ml) (Sigma). Adenovirus-mediated gene transfer of GFP, RGS2, or RGS3 was implemented by adding a minimal volume of the FBS-free MEM containing the gene-carrying adenovirus (100 multiplicities of infection). The full volume of FBS-free MEM was supplied after culture for another 1 to 2 hours. RGS expression and myocyte functional changes were assessed at 24 hours after transfection.

Fluorescence energy resonance transfer studies

Adult myocytes were infected with an adenovirus expressing either the modified EPAC-based cAMP FRET sensor (ICUE3) (14) or SR-localized PKA activity sensor SR-AKAR3 (16). Just before study, cells were washed two times with Hanks' balanced salt solution and imaged at room temperature in the dark. Dual-emission ratio imaging used a 420DF20 excitation filter, a 450DRLP dichroic mirror, and two emission filters (475DF40 for cyan fluorescent protein and 535DF25 for yellow fluorescent protein) and was performed on a Zeiss Axiovert 200 M microscope with a MicroMAX BFT512 cooled charge-coupled device camera (Roper Scientific) controlled by MetaFluor 6.2 software (Universal Imaging). Fluorescent images (taken every 20 to 30 s) were background-corrected by subtracting autofluorescence intensities of untransfected cells (or background with no cells) from the emission intensities of cells expressing reporters.

Human myocardial samples

The catheterization procedures, biopsy protocol, and RNA analysis from human LV myocardial samples have been previously reported (21).

Statistical analysis

Comparisons between multiple experimental groups (no repeated measures) were performed by one-way analysis of variance (ANOVA) with a Tukey multiple-comparison test. In vivo data from the same heart at multiple time points were analyzed by repeated-measures ANOVA. Data are presented as means ± SEM.

Supplementary Material

Refer to Web version on PubMed Central for supplementary material.

Acknowledgments

REFERENCES AND NOTES

1. Lloyd-Jones D, Adams RJ, Brown TM, Carnethon M, Dai S, De Simone G, Ferguson TB, Ford E, Furie K, Gillespie C, Go A, Greenlund K, Haase N, Hailpern S, Ho PM, Howard V, Kissela B, Kittner S, Lackland D, Lisabeth L, Marelli A, McDermott MM, Meigs J, Mozaffarian D, Mussolino M, Nichol G, Roger VL, Rosamond W, Sacco R, Sorlie P, Stafford R, Thom T, Wasserthiel-Smoller S, Wong ND, Wylie-Rosett J. American Heart Association Statistics Committee and Stroke Statistics Subcommittee, Executive summary: Heart disease and stroke statistics—2010 update: A report from the American Heart Association. Circulation. 2010; 121:948–954. [PubMed: 20177011]

2. Cleland JG, Daubert JC, Erdmann E, Freemantle N, Gras D, Kappenberger L, Tavazzi L. Cardiac Resynchronization-Heart Failure (CARE-HF) Study Investigators, The effect of cardiac resynchronization on morbidity and mortality in heart failure. N Engl J Med. 2005; 352:1539–1549. [PubMed: 15753115]

3. Cleland JG, Daubert JC, Erdmann E, Freemantle N, Gras D, Kappenberger L, Tavazzi L. Longer-term effects of cardiac resynchronization therapy on mortality in heart failure [the CArdiac REsynchronization-Heart Failure (CARE-HF) trial extension phase]. Eur Heart J. 2006; 27:1928–1932. [PubMed: 16782715]

4. Bristow MR, Saxon LA, Boehmer J, Krueger S, Kass DA, De Marco T, Carson P, DiCarlo L, DeMets D, White BG, DeVries DW, Feldman AM. Comparison of Medical Therapy, Pacing, and Defibrillation in Heart Failure (COMPANION) Investigators, Cardiac-resynchronization therapy with or without an implantable defibrillator in advanced chronic heart failure. N Engl J Med. 2004; 350:2140–2150. [PubMed: 15152059]

5. Abraham WT, Fisher WG, Smith AL, Delurgio DB, Leon AR, Loh E, Kocovic DZ, Packer M, Clavell AL, Hayes DL, Ellestad M, Trupp RJ, Underwood J, Pickering F, Truex C, McAtee P, Messenger J. MIRACLE Study Group. Multicenter InSync Randomized Clinical Evaluation, Cardiac resynchronization in chronic heart failure. N Engl J Med. 2002; 346:1845–1853. [PubMed: 12063368]

6. Kass DA, Chen CH, Curry C, Talbot M, Berger R, Fetics B, Nevo E. Improved left ventricular mechanics from acute VDD pacing in patients with dilated cardiomyopathy and ventricular conduction delay. Circulation. 1999; 99:1567–1573. [PubMed: 10096932]

7. St John Sutton M, Ghio S, Plappert T, Tavazzi L, Scelsi L, Daubert C, Abraham WT, Gold MR, Hassager C, Herre JM, Linde C. REsynchronization reVErses Remodeling in Systolic left

vEntricular dysfunction (REVERSE) Study Group, Cardiac resynchronization induces major structural and functional reverse remodeling in patients with New York Heart Association class I/II heart failure. Circulation. 2009; 120:1858–1865. [PubMed: 19858419]

8. Ypenburg C, van Bommel RJ, Borleffs CJ, Bleeker GB, Boersma E, Schalij MJ, Bax JJ. Long-term prognosis after cardiac resynchronization therapy is related to the extent of left ventricular reverse remodeling at midterm follow-up. J Am Coll Cardiol. 2009; 53:483–490. [PubMed: 19195605]

9. Barth AS, Aiba T, Halperin V, DiSilvestre D, Chakir K, Colantuoni C, Tunin RS, Dimaano VL, Yu W, Abraham TP, Kass DA, Tomaselli GF. Cardiac resynchronization therapy corrects dyssynchrony-induced regional gene expression changes on a genomic level. Circ Cardiovasc Genet. 2009; 2:371–378. [PubMed: 20031609]

10. Chakir K, Daya SK, Tunin RS, Helm RH, Byrne MJ, Dimaano VL, Lardo AC, Abraham TP, Tomaselli GF, Kass DA. Reversal of global apoptosis and regional stress kinase activation by cardiac resynchronization. Circulation. 2008; 117:1369–1377. [PubMed: 18316490]

11. Chakir K, Daya SK, Aiba T, Tunin RS, Dimaano VL, Abraham TP, Jaques-Robinson KM, Lai EW, Pacak K, Zhu WZ, Xiao RP, Tomaselli GF, Kass DA. Mechanisms of enhanced β-adrenergic reserve from cardiac resynchronization therapy. Circulation. 2009; 119:1231–1240. [PubMed: 19237665]

12. Aiba T, Hesketh GG, Barth AS, Liu T, Daya S, Chakir K, Dimaano VL, Abraham TP, O'Rourke B, Akar FG, Kass DA, Tomaselli GF. Electrophysiological consequences of dyssynchronous heart failure and its restoration by resynchronization therapy. Circulation. 2009; 119:1220–1230. [PubMed: 19237662]

13. Woo AY, Wang TB, Zeng X, Zhu W, Abernethy DR, Wainer IW, Xiao RP. Stereochemistry of an agonist determines coupling preference of β_2-adrenoceptor to different G proteins in cardiomyocytes. Mol Pharmacol. 2009; 75:158–165. [PubMed: 18838481]

14. DiPilato LM, Zhang J. The role of membrane microdomains in shaping β_2-adrenergic receptor-mediated cAMP dynamics. Mol Biosyst. 2009; 5:832–837. [PubMed: 19603118]

15. Kuschel M, Zhou YY, Cheng H, Zhang SJ, Chen Y, Lakatta EG, Xiao RP. G_i protein-mediated functional compartmentalization of cardiac β_2-adrenergic signaling. J Biol Chem. 1999; 274:22048–22052. [PubMed: 10419531]

16. Liu S, Zhang J, Xiang YK. FRET-based direct detection of dynamic protein kinase A activity on the sarcoplasmic reticulum in cardiomyocytes. Biochem Biophys Res Commun. 2011; 404:581–586. [PubMed: 21130738]

17. Xiao RP, Zhang SJ, Chakir K, Avdonin P, Zhu W, Bond RA, Balke CW, Lakatta EG, Cheng H. Enhanced G_i signaling selectively negates β_2-adrenergic receptor (AR)– but not β_1-AR–mediated positive inotropic effect in myocytes from failing rat hearts. Circulation. 2003; 108:1633–1639. [PubMed: 12975249]

18. Gong H, Adamson DL, Ranu HK, Koch WJ, Heubach JF, Ravens U, Zolk O, Harding SE. The effect of Gi-protein inactivation on basal, and β_1-and β_2AR-stimulated contraction of myocytes from transgenic mice overexpressing the β_2-adrenoceptor. Br J Pharmacol. 2000; 131:594–600. [PubMed: 11015312]

19. Rau T, Nose M, Remmers U, Weil J, Weissmüller A, Davia K, Harding S, Peppel K, Koch WJ, Eschenhagen T. Overexpression of wild-type Gαi-2 suppresses β-adrenergic signaling in cardiac myocytes. FASEB J. 2003; 17:523–525. [PubMed: 12631586]

20. Raake PW, Vinge LE, Gao E, Boucher M, Rengo G, Chen X, DeGeorge BR Jr, Matkovich S, Houser SR, Most P, Eckhart AD, Dorn GW II, Koch WJ. G protein–coupled receptor kinase 2 ablation in cardiac myocytes before or after myocardial infarction prevents heart failure. Circ Res. 2008; 103:413–422. [PubMed: 18635825]

21. Vanderheyden M, Mullens W, Delrue L, Goethals M, de Bruyne B, Wijns W, Geelen P, Verstreken S, Wellens F, Bartunek J. Myocardial gene expression in heart failure patients treated with cardiac resynchronization therapy responders versus nonresponders. J Am Coll Cardiol. 2008; 51:129–136. [PubMed: 18191736]

22. Baillie GS, Sood A, McPhee I, Gall I, Perry SJ, Lefkowitz RJ, Houslay MD. β-Arrestin-mediated PDE4 cAMP phosphodiesterase recruitment regulates β-adrenoceptor switching from G_s to G_i. Proc Natl Acad Sci USA. 2003; 100:940–945. [PubMed: 12552097]

23. Kardestuncer T, Wu H, Lim AL, Neer EJ. Cardiac myocytes express mRNA for ten RGS proteins: Changes in RGS mRNA expression in ventricular myocytes and cultured atria. FEBS Lett. 1998; 438:285–288. [PubMed: 9827562]

24. Nunn C, Zou MX, Sobiesiak AJ, Roy AA, Kirshenbaum LA, Chidiac P. RGS2 inhibits β-adrenergic receptor-induced cardiomyocyte hypertrophy. Cell Signal. 2010; 22:1231–1239. [PubMed: 20362664]

25. Takimoto E, Koitabashi N, Hsu S, Ketner EA, Zhang M, Nagayama T, Bedja D, Gabrielson KL, Blanton R, Siderovski DP, Mendelsohn ME, Kass DA. Regulator of G protein signaling 2 mediates cardiac compensation to pressure overload and antihypertrophic effects of PDE5 inhibition in mice. J Clin Invest. 2009; 119:408–420. [PubMed: 19127022]

26. Rogers JH, Tsirka A, Kovacs A, Blumer KJ, Dorn GW II, Muslin AJ. RGS4 reduces contractile dysfunction and hypertrophic gene induction in $G_{\alpha q}$ overexpressing mice. J Mol Cell Cardiol. 2001; 33:209–218. [PubMed: 11162127]

27. Tokudome T, Kishimoto I, Horio T, Arai Y, Schwenke DO, Hino J, Okano I, Kawano Y, Kohno M, Miyazato M, Nakao K, Kangawa K. Regulator of G-protein signaling subtype 4 mediates antihypertrophic effect of locally secreted natriuretic peptides in the heart. Circulation. 2008; 117:2329–2339. [PubMed: 18443239]

28. Yang J, Huang J, Maity B, Gao Z, Lorca RA, Gudmundsson H, Li J, Stewart A, Swaminathan PD, Ibeawuchi SR, Shepherd A, Chen CK, Kutschke W, Mohler PJ, Mohapatra DP, Anderson ME, Fisher RA. RGS6, a modulator of parasympathetic activation in heart. Circ Res. 2010; 107:1345–1349. [PubMed: 20864673]

29. Abramow-Newerly M, Roy AA, Nunn C, Chidiac P. RGS proteins have a signalling complex: Interactions between RGS proteins and GPCRs, effectors, and auxiliary proteins. Cell Signal. 2006; 18:579–591. [PubMed: 16226429]

30. Roy AA, Baragli A, Bernstein LS, Hepler JR, Hébert TE, Chidiac P. RGS2 interacts with Gs and adenylyl cyclase in living cells. Cell Signal. 2006; 18:336–348. [PubMed: 16095880]

31. Sinnarajah S, Dessauer CW, Srikumar D, Chen J, Yuen J, Yilma S, Dennis JC, Morrison EE, Vodyanoy V, Kehrl JH. RGS2 regulates signal transduction in olfactory neurons by attenuating activation of adenylyl cyclase III. Nature. 2001; 409:1051–1055. [PubMed: 11234015]

32. Lan KL, Sarvazyan NA, Taussig R, Mackenzie RG, DiBello PR, Dohlman HG, Neubig RR. A point mutation in $G\alpha_O$ and $G\alpha_{i1}$ blocks interaction with regulator of G protein signaling proteins. J Biol Chem. 1998; 273:12794–12797. [PubMed: 9582306]

33. Zamah AM, Delahunty M, Luttrell LM, Lefkowitz RJ. Protein kinase A-mediated phosphorylation of the β_2-adrenergic receptor regulates its coupling to G_s and G_i. Demonstration in a reconstituted system. J Biol Chem. 2002; 277:31249–31256. [PubMed: 12063255]

34. Chesley A, Lundberg MS, Asai T, Xiao RP, Ohtani S, Lakatta EG, Crow MT. The β_2-adrenergic receptor delivers an antiapoptotic signal to cardiac myocytes through G_i-dependent coupling to phosphatidylinositol 3'-kinase. Circ Res. 2000; 87:1172–1179. [PubMed: 11110775]

35. D'Ascia C, Cittadini A, Monti MG, Riccio G, Saccà L. Effects of biventricular pacing on interstitial remodelling, tumor necrosis factor-α expression, and apoptotic death in failing human myocardium. Eur Heart J. 2006; 27:201–206. [PubMed: 16291773]

36. Wang X, Zeng W, Soyombo AA, Tang W, Ross EM, Barnes AP, Milgram SL, Penninger JM, Allen PB, Greengard P, Muallem S. Spinophilin regulates Ca^{2+} signalling by binding the N-terminal domain of RGS2 and the third intracellular loop of G-protein-coupled receptors. Nat Cell Biol. 2005; 7:405–411. [PubMed: 15793568]

37. Chakir K, Zhu W, Tsang S, Woo AY, Yang D, Wang X, Zeng X, Rhee MH, Mende U, Koitabashi N, Takimoto E, Blumer KJ, Lakatta EG, Kass DA, Xiao RP. RGS2 is a primary terminator of β_2-adrenergic receptor-mediated G_i signaling. J Mol Cell Cardiol. 2011; 50:1000–1007. [PubMed: 21291891]

38. Yuan N, Friedman J, Whaley BS, Clark RB. cAMP-dependent protein kinase and protein kinase C consensus site mutations of the β-adrenergic receptor. Effect on desensitization and stimulation of adenylylcyclase. J Biol Chem. 1994; 269:23032–23038. [PubMed: 8083204]

39. Chuang TT, LeVine H III, De Blasi A. Phosphorylation and activation of β-adrenergic receptor kinase by protein kinase C. J Biol Chem. 1995; 270:18660–18665. [PubMed: 7629197]

40. Vanagt WY, Cornelussen RN, Poulina QP, Blaauw E, Vernooy K, Cleutjens JP, van Bilsen M, Delhaas T, Prinzen FW. Pacing-induced dyssynchrony preconditions rabbit myocardium against ischemia/reperfusion injury. Circulation. 2006; 114:I264–I269. [PubMed: 16820583]

41. Babiker FA, Lorenzen-Schmidt I, Mokelke E, Vanagt WY, Delhaas T, Waltenberger J, Cleutjens JP, Prinzen FW. Long-term protection and mechanism of pacing-induced postconditioning in the heart. Basic Res Cardiol. 2010; 105:523–533. [PubMed: 20336304]

42. Rapti K, Chaanine AH, Hajjar RJ. Targeted gene therapy for the treatment of heart failure. Can J Cardiol. 2011; 27:265–283. [PubMed: 21601767]

43. Pearce N. The use of β agonists and the risk of death and near death from asthma. J Clin Epidemiol. 2009; 62:582–587. [PubMed: 19422997]

44. Zhou YY, Yang D, Zhu WZ, Zhang SJ, Wang DJ, Rohrer DK, Devic E, Kobilka BK, Lakatta EG, Cheng H, Xiao RP. Spontaneous activation of β_2-but not β_1-adrenoceptors expressed in cardiac myocytes from $\beta_1\beta_2$ double knockout mice. Mol Pharmacol. 2000; 58:887–894. [PubMed: 11040034]
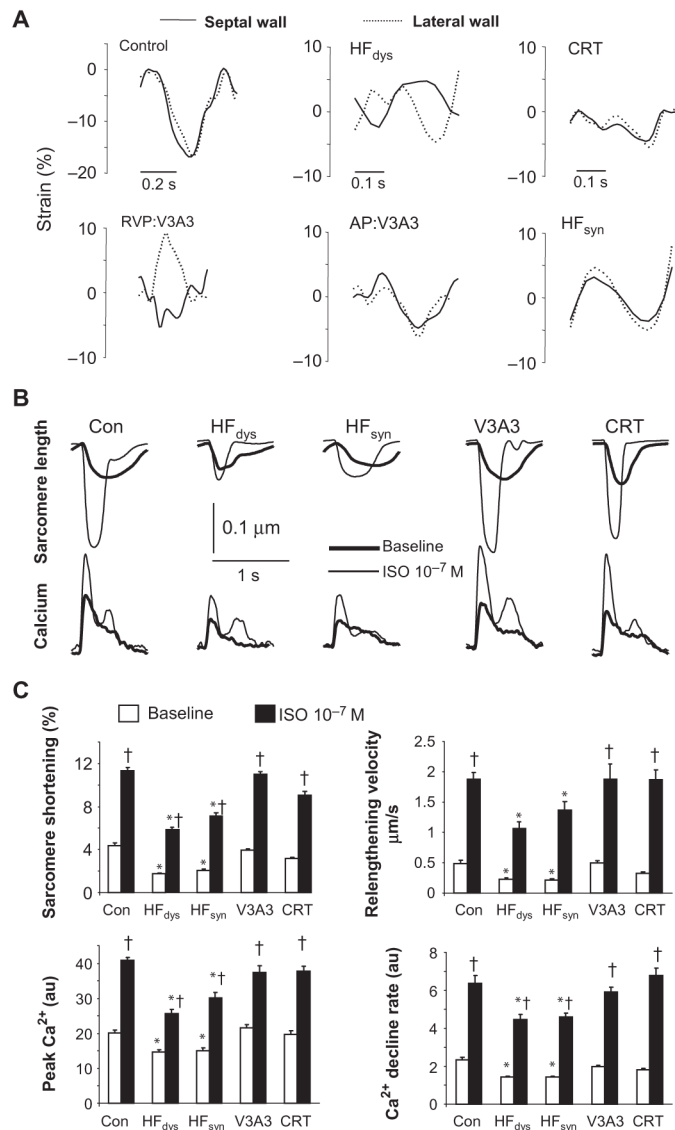
Fig. 1.
Impact of synchronous, dyssynchronous, and resynchronized HF on regional left ventricular wall motion, and myocyte β-adrenergic responsiveness. (**A**) Regional longitudinal strain (derived from speckle tracking) for septal/anterior wall (solid line) and lateral wall (dotted line) of left ventricles in control and HF models. Normal controls have similar, simultaneous strains in both regions. In HF_{dys}, septal shortening precedes the lateral wall, with reciprocal septal stretch when the latter wall contracts. Restoration of synchrony is observed in the CRT model. Synchronous HF (HF_{syn}) displays concurrent strain in both regions. For V3A3, dyssynchrony is observed during the initial 3-week RV pacing period (RVP) and this is reverted to synchronous in the latter atrial pacing period (AP:V3A3). (**B**) Sarcomere shortening and whole-cell calcium transients from isolated myocytes in each model. Data are from cells isolated from the lateral wall, although, as reported, HF_{dys} and CRT models show similar behavior in both anterior and lateral walls (11). Basal function (baseline) and peak calcium transient, as well as their stimulation by isoproterenol (ISO), were equally depressed in HF_{dys} and HF_{syn} models, but enhanced in both resynchronized models (V3A3 and CRT) back to near-control levels. (**C**) Summary results for peak rest and isoproterenol-

stimulated shortening, cell relengthening velocity, peak calcium, and rate of calcium decline ($n = 12$ to 20 cells per heart, $n = 4$ to 5 hearts per group). All of the properties were depressed only in HF$_{dys}$ and HF$_{syn}$ models. *$P < 0.01$ versus all other groups; [†]$P < 0.001$ versus baseline.
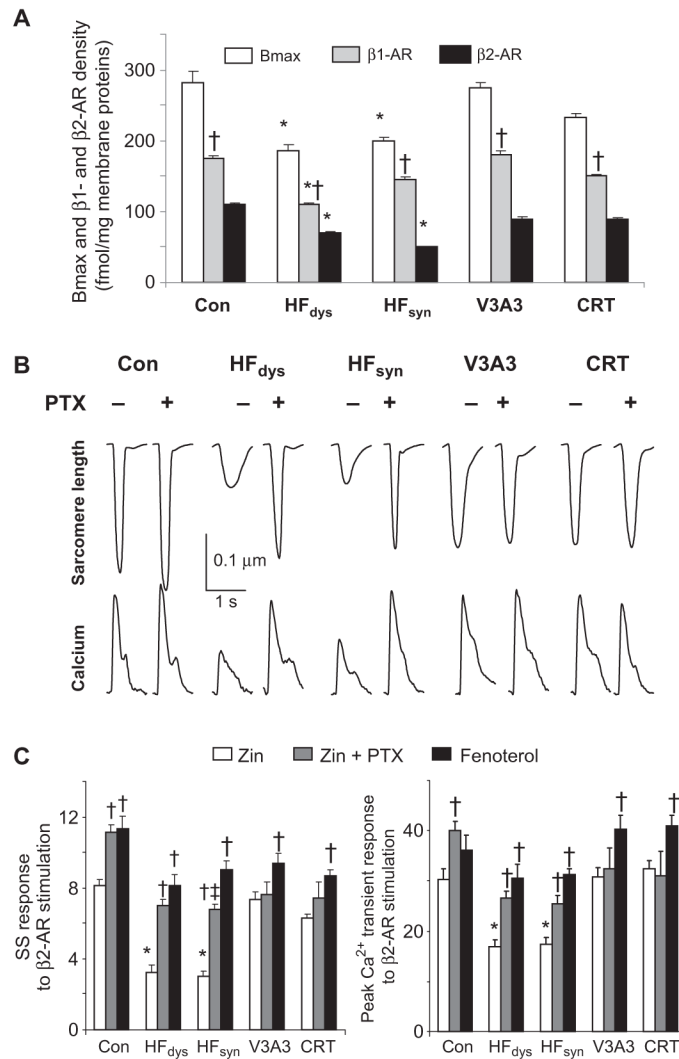
Fig. 2.
Resynchronization enhances β-receptor density and shifts signaling away from $G\alpha_i$ coupling to generate a $G\alpha_s$-biased response. (**A**) β-Receptor maximal affinity binding (Bmax) reflecting surface membrane receptor abundance for combined and individual β_1-AR and β_2-AR subtypes. $n = 4$ for each group. *$P < 0.05$ versus other HF groups and control (within respective receptor group); †$P < 0.01$ versus β_2-AR response. (**B**) Sarcomere shortening (%SS) and whole-cell calcium transient in cells from different models when stimulated with isoproterenol without or with pretreatment by pertussis toxin (PTX). PTX treatment greatly enhanced both behaviors in HF_{dys} and HF_{syn}, but had no impact in resynchronized models. (**C**) %SS and peak Ca^{2+} transient in cells exposed to β_2-AR–selective agonist zinterol (ZIN), zinterol + PTX, or the G_s-biased β_2 agonist fenoterol. $n = 12$ to 20 cells per heart, and 3 to 4 hearts per group. *$P < 0.01$ versus other groups; †$P < 0.001$ versus zinterol; ‡$P < 0.001$ versus fenoterol.
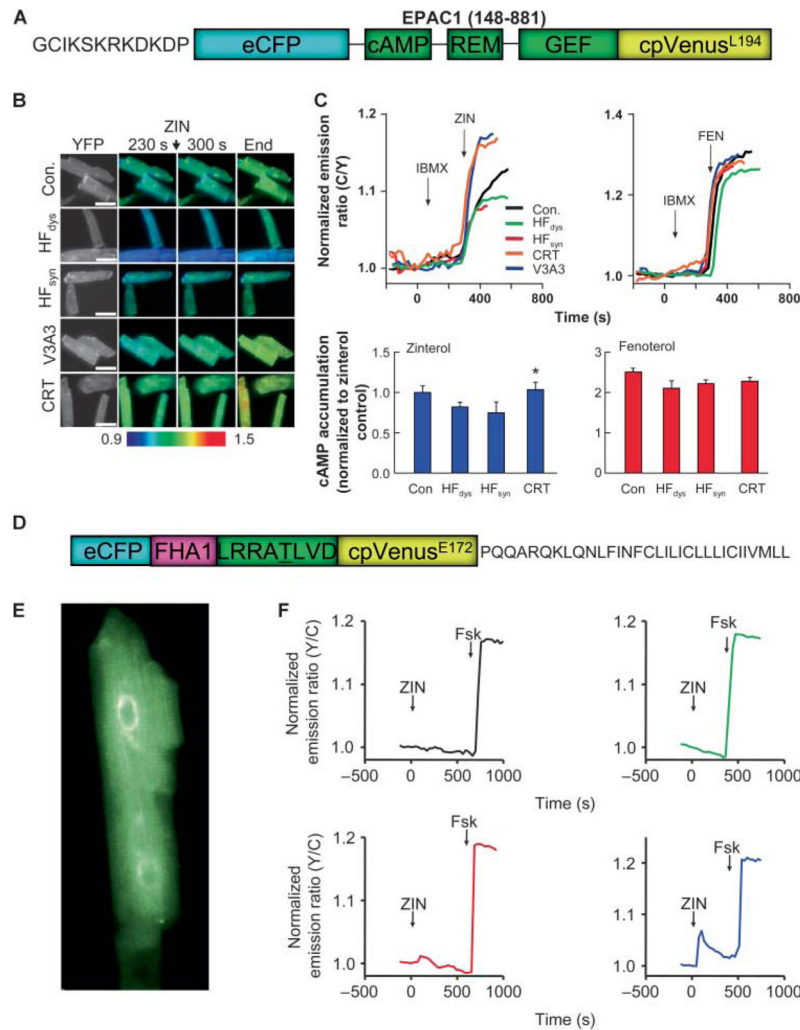
Fig. 3.
Resynchronization enhances myocyte cAMP levels and PKA activation in the SR in response to β_2 stimulation. (**A**) Domain structure of ICUE3 FRET probe for analysis of membrane-localized cAMP generation. Cells were studied in the presence of IBMX to inhibit PDEs and stimulated with either zinterol or fenoterol. (**B**) Example of cell fluorescence ratio–encoded images from myocytes in each group, showing enhanced cAMP generated in CRT models stimulated by zinterol. (**C**) Upper panels show time tracings for FRET ratio in cells stimulated with zinterol or fenoterol, and lower panels summarize data from all experiments (n = 8 to 15 per group). Zinterol induced a greater response in CRT models, whereas fenoterol led to a similarly elevated response in all groups. (**D**) Domain structure of SR-AKAR3 FRET probe used for sarcoplasmic reticulum (SR)-localized PKA activity. (**E**) Myocyte expressing SR-AKAR3 shows fluorescence in tubular SR throughout the cell. (**F**) Example time tracings of SR-AKAR3 FRET in cells treated with zinterol. Only myocytes from CRT models showed PKA activation in the SR. Forskolin (Fsk) is used as a positive control showing functionality of the probe after direct AC stimulation (n = 4 to 5 per group).
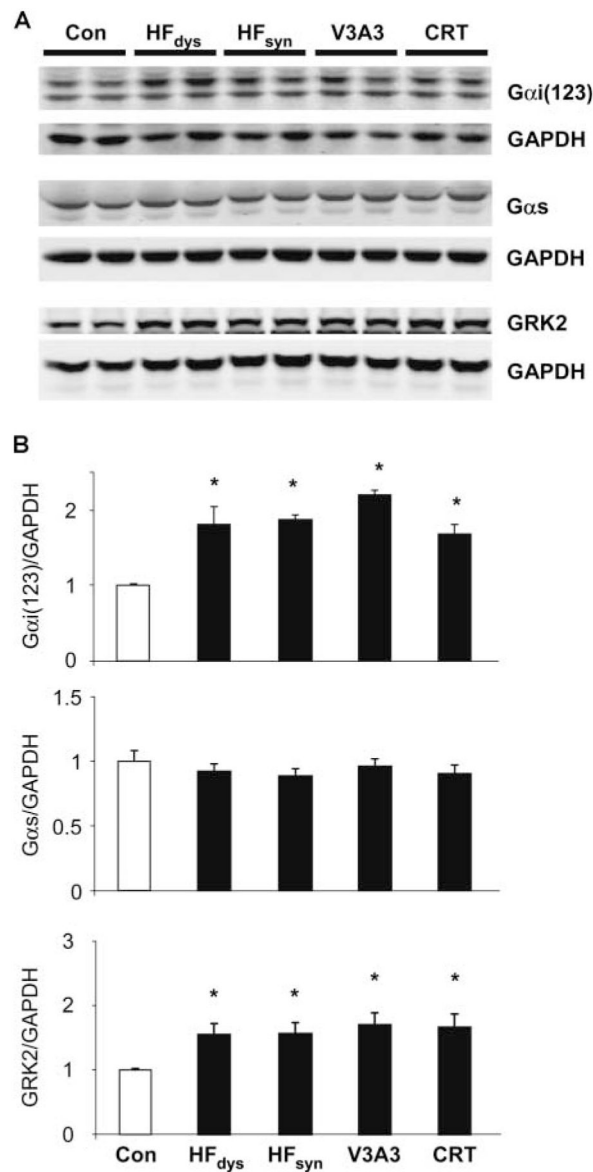
Fig. 4.
Protein expression of $G\alpha_i$ and GRK2 but not $G\alpha_s$ increases in each HF model over control. (**A** and **B**) Western blots (A) and summary densitometry (B) for protein levels of $G\alpha_i(1,2,3)$, $G\alpha_s$, and GRK2 ($n = 4$ to 5 per group). Analysis is normalized to GAPDH as a loading control. *$P < 0.05$ versus control.
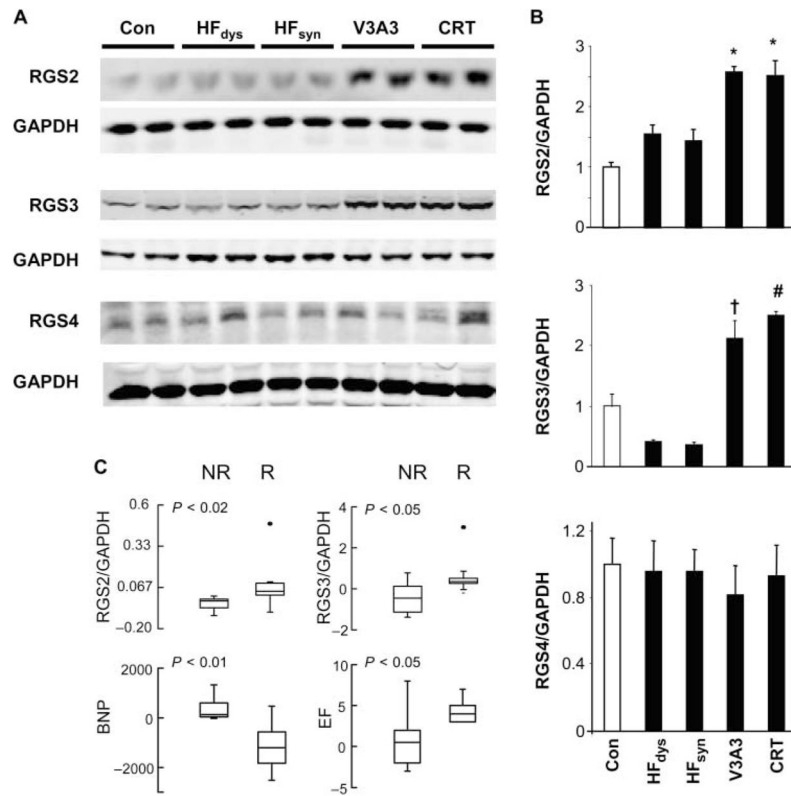
Fig. 5.
Up-regulation of RGS2 and RGS3 in canine models of resynchronization and human responders to chronic CRT. (**A** and **B**) Western blots (A) and summary densitometry (B) for protein expression of RGS2, RGS3, and RGS4 ($n = 4$ to 5 per group). Analysis is normalized to GAPDH as a loading control. *$P < 0.001$ versus control (Con); $P < 0.01$ versus HF$_{dys}$ and HF$_{syn}$; †$P < 0.01$ versus control; $P < 0.001$ versus HF$_{dys}$ and HF$_{syn}$; #$P < 0.001$ versus all other groups. (**C**) Enhanced RGS2 and RGS3 mRNA expression is present in human LV biopsy samples from responder (R) patients, whereas it is absent in nonresponders (NR). Responders also demonstrated a significant decline in myocardial B-type natriuretic peptide (BNP). Differential response in EF is also displayed for the two groups.
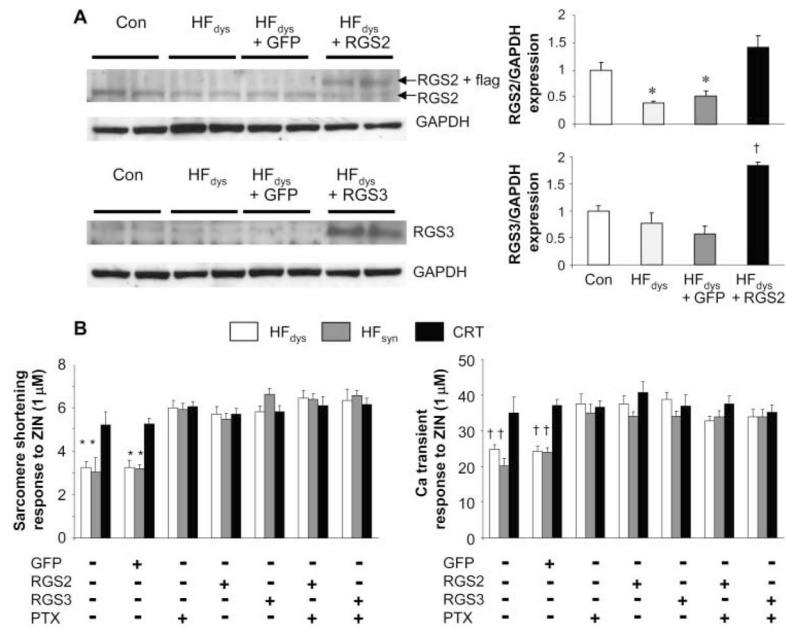
Fig. 6.
Up-regulation of RGS2 or RGS3 in HF_{dys} myocytes is sufficient to convert the β_2-adrenergic stimulation phenotype to that of CRT (or V3A3) responses. (**A**) Isolated myocytes from HF_{dys} hearts were exposed to adenovirus with either GFP (control) or RGS2 or RGS3 vectors. Up-regulation of protein was confirmed in the myocytes and was in the range of 50 to 60% over controls. Adenovirus-GFP controls were similar to noninfected HF_{dys} cells. *$P < 0.05$ versus control and HF_{dys}; †$P < 0.05$ versus other groups. (**B**) Summary data showing sarcomere shortening response to zinterol in myocytes from HF_{dys}, HF_{syn}, or CRT hearts after 24-hour infection with adenovirus containing GFP or full-length RGS2 or RGS3. Data are also shown with or without concomitant PTX treatment. $n = 12$ to 18 cells per heart, $n = 2$ to 3 hearts per group. *$P < 0.01$ versus CRT; †$P < 0.001$ versus CRT.
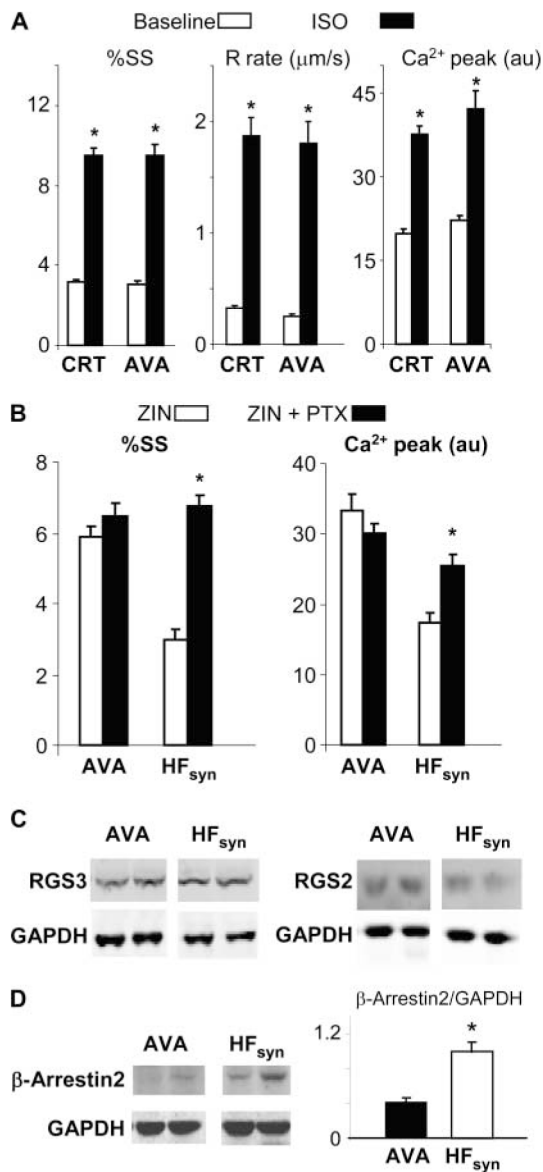
Fig. 7.
Enhanced β-AR responsiveness in myocytes from hearts exposed to RV (dyssynchrony) pacing during the middle 2 weeks of otherwise 6-week atrial tachypacing (AVA). (**A**) %SS and peak Ca^{2+} transients are similar at baseline and after isoproterenol stimulation in myocytes from an AVA heart to those observed after CRT. *$P < 0.001$ versus baseline (nonstimulated). (**B**) Minimal augmentation of functional or Ca^{2+} response to zinterol in AVA myocytes by addition of PTX. Data are compared with the HF_{syn} model, which displayed marked augmentation. *$P < 0.05$ versus zinterol alone. $n = 12$ to 20 cells per heart, $n = 4$ hearts for each group. (**C**) Protein expression for RGS3 and RGS2 in AVA model, shown in comparison with the HF_{syn} model. There was no up-regulation in this model, unlike CRT ($n = 4$ to 5 per model). (**D**) Protein expression (left) and summary densitometry (right) for β-arrestin2, shown in comparison to HF_{syn} data. Unlike HF_{syn}, which had no change in expression over control or the other models (fig. S4), AVA myocytes had very low levels. *$P < 0.001$.